Ultrasound and Deep Eutectic Solvents: an efficient combination to tune the mechanism of steviol glycosides extraction

Gualtiero Milani[a,*], Maryline Vian[b], Maria Maddalena Cavalluzzi[a], Carlo Franchini[a], Filomena Corbo[a], Giovanni Lentini[a], and Farid Chemat[b]

[a] Department of Pharmacy-Pharmaceutical Sciences, University Aldo Moro-Bari, Via Orabona, 4, 70126 Bari, Italy

[b] Avignon University, INRA, UMR408, GREEN Extraction Team, 84000 Avignon, France

Corresponding author: Gualtiero Milani

e-mail address: gualtiero.milani@uniba.it

Abstract:

Ultrasound-assisted extraction is widely recognized as an eco-friendly technique due to low solvent consumption and time extraction as well as enhanced extraction efficiency with respect to conventional methods. Nevertheless, it would be convenient to avoid the usually used organic solvents to reduce the environment pollution. In this regard, Deep Eutectic Solvents (DES) represent nowadays a green and sustainable alternative for the extraction of bioactive compounds from natural sources. In this study, an efficient extraction of stevioside and rebaudioside A from *Stevia rebaudiana* coupling ultrasound with DES was developed. A solvent screening was performed using the predictive approach COnductor-like Screening MOdel for Real Solvent (COSMO-RS). The effect of three independent variables, namely % of water, temperature, and sonication amplitude, were investigated by the response surface methodology (RSM). Comparing ultrasound-assisted extraction (UAE) with conventional extraction, it has been demonstrated that the amount of steviol glycosides through UAE is almost three times higher than that obtained by the conventional method. Possible physicochemical factors involved in the UAE mechanism were discussed.

Keywords: *Stevia rebaudiana*, Ultrasound, Deep Eutectic Solvents, COSMO-RS, Green Extraction.

Abbreviations: **CCD**, Central Composite Design; **CER,** constant extraction rate period; **COSMO-RS**, COnductor-like Screen MOdelfor Real Solvent; **DC,** diffusion-controlled rate period; **DEEAC**, *N,N*-diethyl ethanol ammonium chloride; **DES**, Deep Eutectic Solvent; **DFT**, density functional theory; **EG**, Ethylene glycol; **FER,** falling extraction rate period; **Gly**, glycerol; **HBA**, Hydrogen Bond Acceptor; **HBD**, Hydrogen Bond Donor; **HPTLC**, High Performance Thin Layer Chromatography; **LA**, levulinic acid; **N-HBA**, Non-Hydrogen Bond Acceptor; **N-HBD**, Non-Hydrogen Bond Donor; **RSM**, Response Surface methodology; **TBAB**, tetrabutylammonium bromide; **TBAC**, tetrabutylammonium chloride; **TEG**, triehylene glycol; **TEAB**, tetraethylammonium bromide; **TEAC**, tetraethylammonium chloride; **TPAB**, tetrapropylammonium bromide; **TZVP**, triple ζ valence potential; **UAE**, Ultrasound-Assisted Extraction.

1. Introduction

Stevia rebaudiana Bertoni, botanically classified in 1899 by Moisès Santiago Bertoni, is a perennial semi-shrub of the *Asteraceae* family, native to Paraguay. Today its cultivation is widespread in almost all regions of the world including Europe, Canada, and Asia. In *Stevia rebaudiana* leaves are present more than 30 glycosides of the diterpenic carboxylic alcohol steviol (13-hydroxy-*ent*-kaur-16-en-19-oic acid), among which stevioside and rebaudioside A are the most abundant. Although their concentrations depend on the genotype and cultivation conditions, the values usually found in dried leaves are 4–13% for stevioside and 2–4% for rebaudioside A [1,2]. They are responsible for the *Stevia* sweet taste, having sweetening power about 250 and 450 times higher than saccharose, respectively. Other steviol glycosides are present in smaller quantities in the leaves and include rebaudioside B, C, D, E, F, dulcoside A, and steviolbioside [3,4]. In general, different therapeutic benefits such as

antibacterial, anti-inflammatory, hypotensive, diuretic, and anti-tumors effects are associated with *Stevia rebaudiana* glycosides [4,5]. Interestingly, steviol glycosides can induce pancreas production of insulin thus resulting useful in the treatment of diabetes mellitus. Most of the natural products on the market having functional properties such as sweetening, antioxidant, antibacterial, and antidiabetic, are obtained through extractive processes. Therefore, convenient green extraction methods are required to obtain healthy food products. In recent years, the extractive scenario has changed leading to a reduction in solvent and energy consumption, as well as promoting the use of alternative solvents, anyway providing a high extractive yield of the target compounds. Several innovative techniques have been applied in different fields such as nutraceutical, pharmaceutical, food, and cosmetic production. They include ultrasound extraction, supercritical fluid extraction, subcritical water extraction, pulse electric field, controlled pressure drop process, and microwave extraction [6–10].

In the last decade, ultrasounds have been successfully applied not only to inorganic and medicinal chemistry but also in the food industry [11–14]. Ultrasonic waves accelerate the extraction process through the cavitation phenomena that generate high-speed micro-jets inducing fragmentation, erosion, and sonoporation of the solid matrix surfaces, thus improving the mass transfer process. However, several parameters can greatly affect the ultrasound-assisted extraction (UAE) process such as solvent composition, temperature, presence of dissolved gases, sonication time, particle size of the raw material, and matrix parameters [15]. Unfortunately, organic solvents with high level of toxicity, volatility, and flammability are often required and, to overcome these drawbacks, Deep Eutectic Solvents (DESs) have been proposed as green and sustainable alternative on the basis of the six principles of green extraction. DESs have emerged as a new generation of ionic liquids synthesized by combining a hydrogen bond acceptor (HBA) and a hydrogen bond donor (HBD) [16]. Thermal stability, low vapor pressure, non-flammability, low toxicity, and

water-solubility make them green solvents, while being also cheap and easy to prepare [7,17–19]. Recently, DES were successfully used in the extraction of various kind of bioactive compounds from different plant materials [20–22]. This study aimed to develop a new green DES-UAE method for the extraction of stevioside and rebaudioside A from *Stevia rebaudiana* leaves. The choice of the best extraction solvent was made using the computational prediction software COSMO-RS, which allowed for calculating the theoretical value of the solubility index of target steviol glycosides in different solvents. The recovery yields of stevioside and Rebaudioside A content were determined using HPTLC as the analytical method.

2. Materials and methods

2.1 Plant material and chemicals

Dry leaves of *Stevia rebaudiana* were obtained from Stevia Natura (Riom, France). Their initial dry matter content was 0.92 ± 0.04 g per 1g of dry leaves determined by a moisture balance (Ohaus, model MB 35). Ethylene glycol, ethyl acetate (HPLC grade), methanol (HPLC grade), acetic acid, sulfuric acid were purchased from Merck KGaA. Absolute ethanol, methanol, and water (HPLC grade) were purchased from VWR international (Leuven, Belgium). Tetraethylammonium chloride was purchased from TCI EUROPE N.V. (France). Stevioside (analytical standard) and rebaudioside A (analytical standard) were purchased from Extrasynthese S.A. (Genay, France).

2.2 Preparation of DESs

Tetraethylammonium chloride (TEAC) was used as the HBA, while ethylene glycol (EG) was used as the HBD. DES was prepared by heating the mixture, as previously describes by Warrag et al. [23]. In brief, TEAC was mixed with EG at 1:2 molar ratio, then heated to 82 °C with constant agitation until a clear, homogeneous, and stable liquid was formed.

2.3 COSMO-RS model and computational details

Geometry optimization was run on HBA [choline chloride (ChCl), *N*,*N*-diethyl ethanol ammonium chloride (DEEAC), tetraethylammonium chloride (TEAC), tetraethylammonium bromide (TEAB), tetrapropylammonium bromide (TPAB), tetrabutylammonium chloride (TBAC), tetrabutylammonium bromide (TBAB)], HBD [glycerol (Gly), levulinic acid (LA), ethylene glycol (EG), triethylene glycol (TEG)], and steviol glycosides (stevioside, rebaudioside A, rebaudioside B, rebaudioside C, rebaudioside D, rebaudioside E, rebaudioside F). The initial structure of each HBA and HBD was drawn by TURBOMOLE software (TmoleX license version 7.4 COSMOlogic GmbH &Co. KG) and geometry optimization was performed at the Hartree-Fock level by using the 6-31G* basis set [def-SV(P)]. From the optimized geometry of each HBD and HBA the corresponding **.cosmo file** was generated using the density functional theory (DFT) combined with Becke-Perdew functional and triple ζ valence potential (TZVP) basis set. All of these tasks were performed with the Turbomole software package. Thereafter, the **.cosmo files** were imported into the COSMOthermX software (COSMO thermX, licese version 19.0, COSMOlogic GmbH &Co. KG) package with the parameterization file BP_TZVP_18.ctd [24]. For each steviol glycoside the corresponding **.cosmofile** was generated in COSMOthermX program using DFT combined with Becke-Perdew functional and TZVP basis set. The σ-surface, σ-profiles, σ-potentials, and the affinity between the solute and the solvents were retrieved from COSMOthermX. The affinity of the solvent to the solute can be associated to the σ-potential. In this work, the model is based on the prediction of the chemical potential of each solute in 26 different DESs. The absolute solubility of target steviol glycosides was calculated with COSMOthermX software as follows:

$$\log_{10}(x_j) = \log_{10}[\exp(\mu_j^{pure} - \mu_j^{solvent} - \Delta G_{j,fusion})/RT)]$$

where: μj^{pure} is the chemical potential of pure compound j (J/mol); $\mu j^{solvent}$ is the chemical potential of solvent j at infinite dilution (J/mol); $\Delta G_{j,fusion}$ is the free energy of fusion of

compound j (J/mol); x_j solubility of compound j (g/g solvent). The logarithm of the best solubility is set to 0 and all other solvents are ranked relatively to the best or reference solvent [25]. Figure 1 summarizes the theoretical steps performed for the calculation of solubility in COSMO-RS.

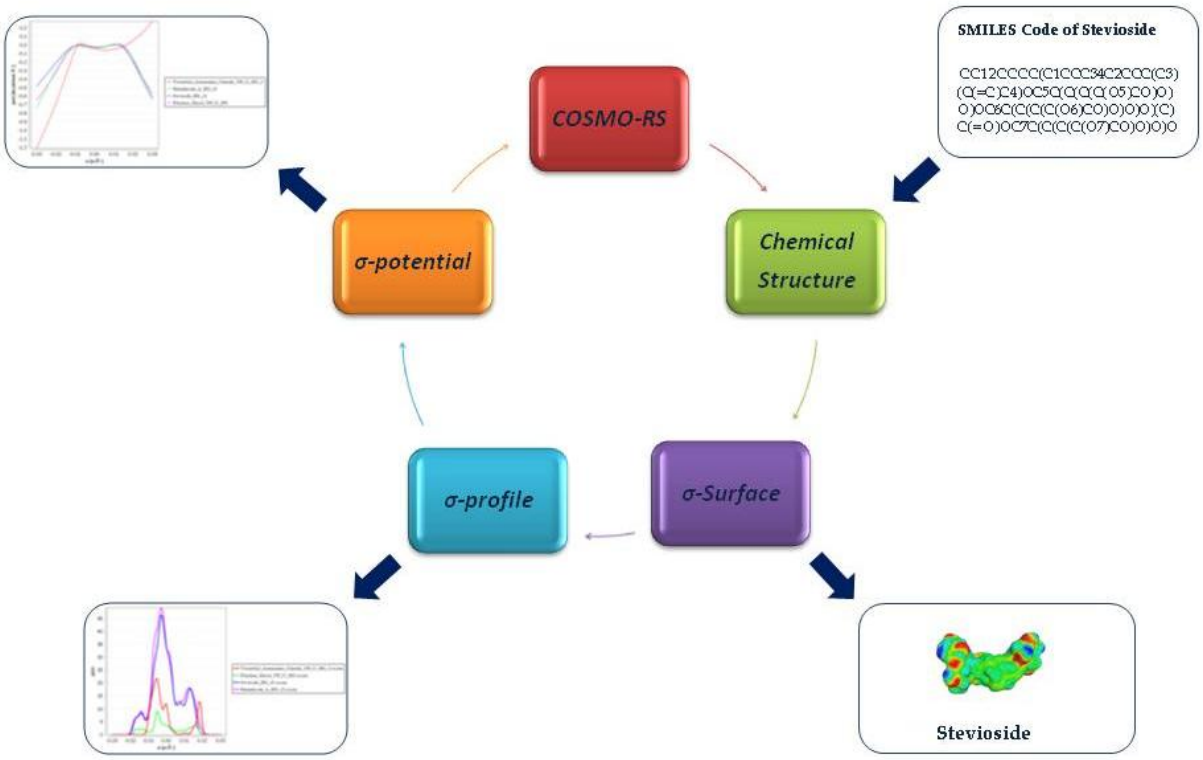

Figure 1. Representative image for theoretical solubility prediction using COSMO-RS.

2.4 Instrumentation

2.4.1 Sonication apparatus

Sonication was achieved at low frequencies of 20 kHz. UAE experiments were performed in a cylindrical glass reactor (volume 200 mL) connected to a heating/cooling system (Huber, Germany). A Vibracell 75186 ultrasonic generator fitted with an immersible probe emits the sound vibration into the solution via a titanium alloy rod (5 mm) placed in the liquid, in the middle of the mixture, with a total supplied power input of 130 W.

2.4.2 High Performance Thin Layer Chromatography Analysis

The samples and standards were spotted in the form of bands of 8 mm width with a Camag microliter syringe controlled by the Automatic TLC Sampler ATS 4 (Camag, Muttenz, Switzerland) on precoated silica gel glass Plate 60 Å F254 (20 × 10 cm; Merck, Darmstadt, Germany). The plates were prewashed by methanol and activated at 100 °C for 30 min on the TLC plate heater (CAMAG, Muttenz, Switzerland) prior to spotting. The chromatogram was developed in an Automatic Development Chamber ADC2 (Camag, Muttenz, Switzerland) with a mixture of ethyl acetate/methanol/acetic acid (3:1:1, v/v/v) as a mobile phase. The spots were visualized by dipping the plate in a solution of acetic acid/sulfuric acid/absolute ethanol (1:1:10, v/v/v) then heated at 120 °C for 15 min on a TLC plate heater. The densitometric analysis was performed on CAMAG TLC Scanner 3. The scanning was performed at 500 nm in reflectance/absorption mode. Visualizer documentation system was used to take image of the TLC plate under the white light. Standard solutions of stevioside and rebaudioside A were prepared by solubilizing 10 mg of each standard compound in 10 mL of methanol. The calibration of the method was performed by spotting increasing volumes of each standard solution to obtain six concentrations in the range 0.1–2 µg/spot. Stevioside and rebaudioside A quantification was performed in duplicate and all the recorded data were processed with WinCATS software (V 1.4.7.2018, Camag, Muttenz, Switzerland). The final results are expressed as the mean value ± SEM of three experiments for each analysis.

2.5 Extraction procedures

2.5.1 Kinetic study

A preliminary kinetic study was performed in a cylindrical glass reactor where 7 g of *Stevia* leaves were macerated at 25 °C in 70 mL of solvent. A magnetic stir bar was used to ensure homogenization of the mixture at 450 rpm during all the experiments. In order to follow the

kinetic, 1 mL of sample was collected from the reactor after 5, 10, 15, 30, 40, 60, and 90 min. The sample was transferred into a 2 mL microtube and centrifuged at 8875 g for 10 min (Sigma 4-16KS). The suspension was diluted in methanol and filtered through a 0.45 μm PTFE filter and stored at – 20 °C for subsequent analysis. Each extraction was performed in triplicate.

2.5.2 Ultrasound-assisted extraction

Seven grams of dried leaves were poured in 70 mL of solvent and extracted with ultrasonic device in 40 min. Throughout the sonication, a magnetic stir bar was used to ensure uniform absorption of ultrasonic energy and medium homogeneity. The sample was transferred into a 2 mL microtube and centrifuged at 8875 g for 10 min. The suspension was diluted in methanol and filtered through a 0.45 μm PTFE filter and stored at –20 °C for subsequent analysis. Extraction experiments were made in triplicate (except for the experimental design).

2.5.3 Conventional extraction

Conventional extraction was carried out in the same conditions as above but without ultrasound. All experiments were carried out in triplicate.

2.6 Experimental design study

The investigation of the performance of UAE and the optimization of extraction parameters were performed by a response surface methodology (RSM) using the software STATGRAPHICS PLUS (Rockville, USA, 2000). Central composite design (CCD), also called Box-Wilson design, was used to evaluate the relevance and interaction of the three controlled factors in the extraction process, namely % of water, temperature, and sonication amplitude. This multivariate study provides a complete exploration of the experimental domain using a two-level full factorial design (coded ± 1), superimposed by center points (coded 0) and star points (coded ± α) located on variable axes at a distance α from the centre, thus establishing new extremes for the parameters of the factors involved, for a total of 20

experiments. The selected optimization responses were the concentrations of stevioside (Y_1, mg/g dried leaves) and rebaudioside A (Y_2, mg/g dried leaves). An analysis of variance (ANOVA) with 95% confidence level was then carried out for each response variable in order to determine the validity of the model.

2.7 Determination of ultrasound physical impact: localized sonication

To evaluate the impact of ultrasounds on *Stevia* leave extraction yields, appropriately selected dry leaves were subjected to sonication at the operating conditions predicted by CCD. All the selected leaves (1.5 cm width, 5 cm length) were fixed in a perforated disk with a central opening diameter of 1 cm. The disk was introduced in a cylindrical glass reactor (volume 500 mL) connected to a heating/cooling system (Huber, Germany) to maintain the temperature at 59.4 ± 1 °C. 300 mL of a TEAC:EG with 10% of water were then added. Localized sonication was achieved using the ultrasonic probe, fixed at the distance of 0.5 cm from the leaf. All experiments were carried out with 90% of the amplitude generated from the probe. Different duration (times) of sonication (30 sec, 1 min, 3 min) were investigated to highlight the ultrasound physical impact during the treatment. Untreated and treated leaves were subsequently analyzed by macroscopic technique. All experiments were carried out in triplicate.

2.8 Macroscopic analysis

To visualize the impact of ultrasound, sonicated and non-sonicated leaves were fixed on a microscope slide and were analyzed using a stereomiscoscope (Leica EZ4, Leica Microsystems, Germany) with a magnification of 0.68. All experiments were carried out in triplicate.

2.9 Determination of contact angles

To determine the contact angles of different solvents, a drop (5 µL) was gently dispensed on the surface of the dry leaf (1cm width, 5 cm length), previously fixed on a microscope slide

by a syringe (Agilent, 5162-9600). The contact angle was measured through an image analysis, using a camera (Nikon) arranged from the microscope slide to 20 cm (magnification 20X) and the contact angle was calculated by a goniometer. All experiments were carried out in triplicate.

3. Results and discussion

3.1 Solvent screening: COSMO-RS simulation

Nowadays, solvents and mixtures available for extraction processes are numerous as well as the computational theoretical models which represent a valuable resource for the estimation of the thermodynamic properties of solutions and mixtures. Through these calculations, it is possible to reduce resources, time, and spending needed to find the best extraction solvent at the initial stage of solvent skimming in the laboratory. COnductor-like Screening MOdel for Real Solvent (generally known as COSMO-RS), one of the most widely used computational theoretical models [26,27], has been chosen in our study. It is well-known that DESs can be prepared by mixing and heating at about 80 °C a suitable HBA and HBD. A mixture with a large depression of the melting point, which results lower than those of the single constituents, is obtained. Generally, quaternary ammonium salt possesses HBA properties, while alcohol, carboxylic acids, amines, ureas, or carbohydrates possess HBD properties. Twenty-six different DESs (resulting from the combination of seven HBAs and four HBDs) were selected among those reported in the literature and the computational study was carried out on seven representative glycosides contained in the *Stevia* leaves (stevioside, rebaudioside A, B, C, D, E, F)[28–30]. The used molar ratios are reported in Figure S1 (Supplementary Material). In COSMO-RS, σ-profile (Figure 2) provides information about the molecular polarity distribution. For example, the broad peaks around –0.015 e/Å^2 identify the H atoms of the alcoholic groups of stevioside or EG, whilst the narrow distribution of the charge densities around zero identifies the aliphatic chain of diterpene groups. Finally, all the

overlapping peaks at about +0.02 e/Å^2 are related to chloride or bromide ions of the considered ammonium salt. Similar information can be achieved by the σ-potential analysis (Figure 3). In general, negative **μ(σ)** values indicate HBA and HBD proprieties, in the left and right quadrant, respectively. Conversely, non-HBA (N-HBA) and non-HBD (N-HBD) groups are included in the upper left and right quadrants, respectively, having positive **μ(σ)** values.

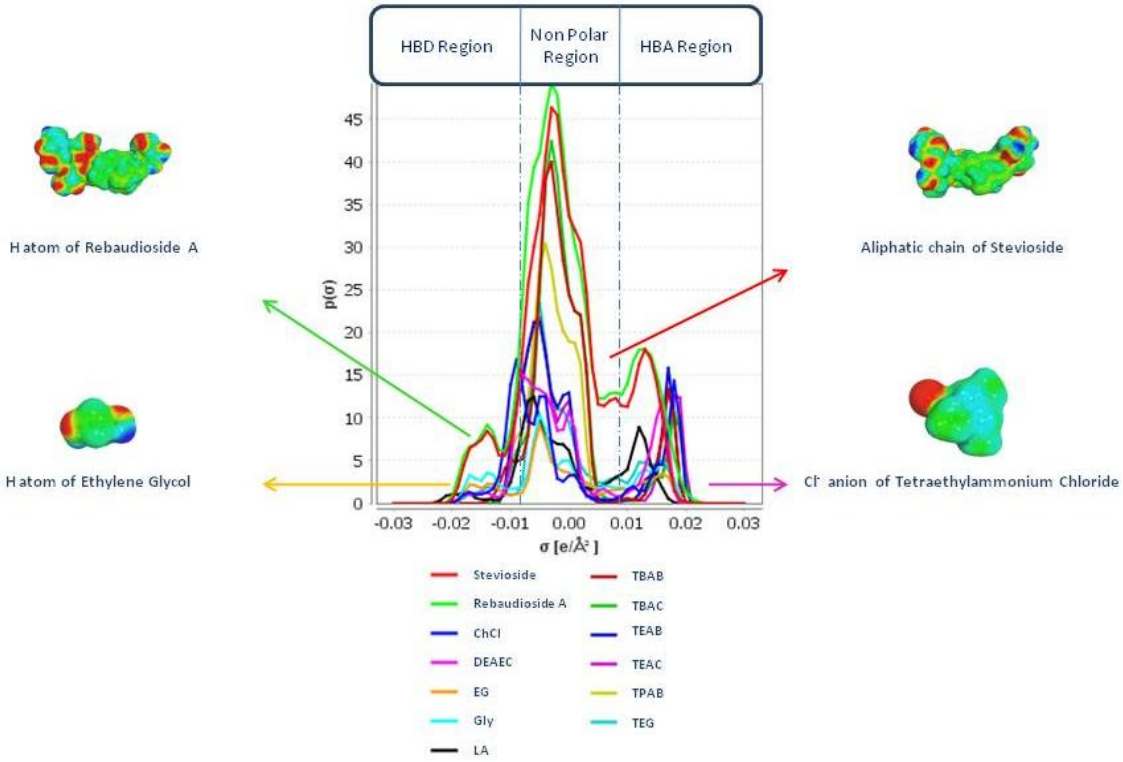

Figure 2. σ-profile of selected solutes and solvents calculated using COSMO-RS.

As concerns the compounds selected for our study, a symmetric shape of σ-potential (Figure 3) has been obtained in the lower quadrants for steviol glycosides, EG, TEG, GLY, LA, all having both HBA and HBD proprieties. Conversely, ammonium salts such as TEAC, TEAB, TPAB, TBAC, and TBAB, which possess only HBA properties, showed an asymmetric trend from the HBA to the N-HBD quadrant. The absolute solubility values, expressed in $\log_{10}(x_j)$ and calculated for the selected solutes (stevioside, rebaudioside A, B, C, D, E, F) in the 26 DESs chosen for the study, are reported

in Figure 4. A color scale with values ranging from – 1 to – 10 has been generated with values included between – 1 and – 4, depicted in green chromatic scale, indicating high solubility indices. The results of COSMO-RS simulations show that the pair TEAC:EG is the best pair among all the combinations of HBAs and HBDs for all the steviol glycosides. Therefore, it was chosen to carry out the extraction process and our attention was focused in particular on the recovery of stevioside and Rebaudioside A, which are notoriously the most abundant metabolites in *Stevia* leaves.

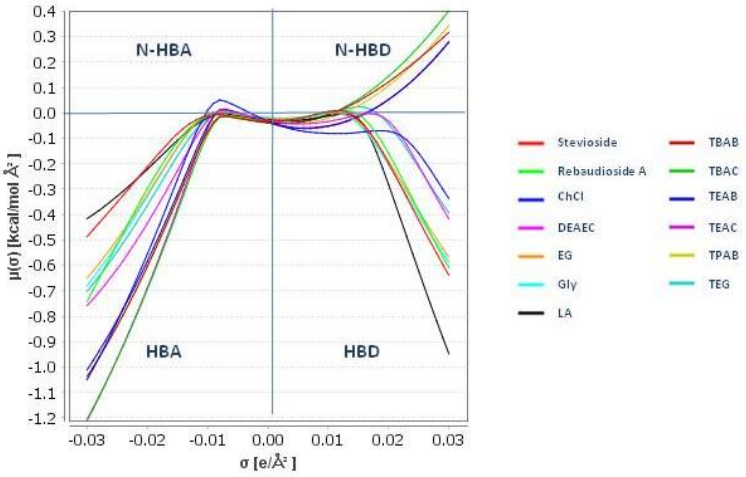

Figure 3. σ-potential of select solutes and solvents calculated using COSMO-RS.

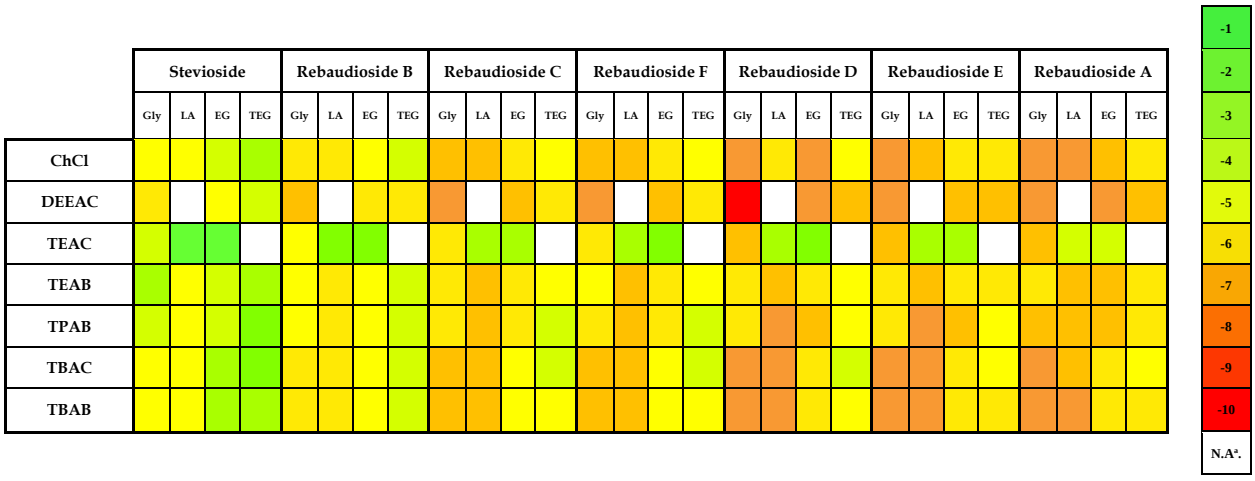

Figure 4. COSMO-RS predicted solubilities of steviol glycosides in 26 DESs at 25 °C. [a] **N.A.:** Not available. Values included between – 1 and – 4, depicted in green chromatic scale, indicate high solubility indices. Values included between – 5 and –7, depicted in yellow chromatic scale, indicate medium solubility indices. Values included between – 8 and – 10, depicted in red chromatic scale, indicate lower solubility indices.

3.2 Kinetic study

At first, to evaluate the interaction between solvent and solute surface, solvent diffusion, solute diffusion, and solute transfer outside the matrix surface, a kinetic study was performed by conventional extraction [6]. Forecasting the difficulties we would have encountered in the UAE step due to the high TEAC:EG viscosity, this preliminary study was performed using DES plus 50% water. Quantitative analysis of extracted steviol glycosides was performed at different extraction times by HPTLC (Figure 5). The kinetic results obtained are depicted in Figure 6 and the corresponding values are reported in Table S2 (Supplementary Materials). The two glycosides were extracted to the same extent regardless of time of observation, with the maximum value reached at 90 min (30 ± 5 mg/g and 30 ± 6 mg/g for stevioside and rebaudioside A, respectively). On the other hand, the plateau observed after 40 minutes indicates that the extraction process could be stopped at this time since the metabolites are completely extracted from the plant.

The kinetic study performed using TEAC:EG as such gave no detectable quantity of the two metabolites in the HPTLC analysis, thus indicating the need to use a certain amount of water to extract steviol glycosides from *Stevia* leaves.

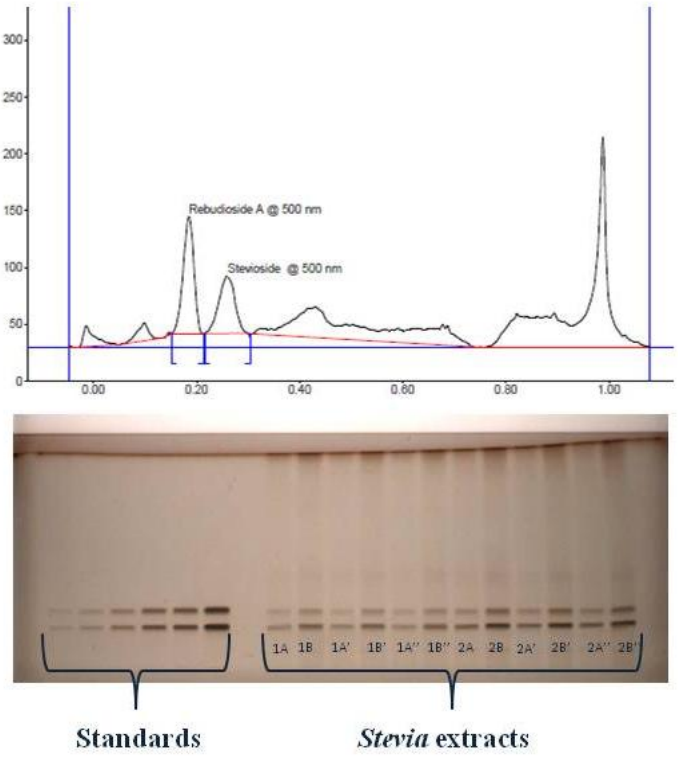

Figure 5. HPTLC chromatogram of *Stevia* extract documented under white light illumination (down) and the densitogram at 500 nm (up). Tracks from left to right: 0.1, 0.2, 0.4, 0.8, 1, 2 μg/spot for both standards; *Stevia* extracts (5 μL/spot) after 60 min (1) and 90 min (2) diluted 40 (A) and 20 (B) times, respectively.

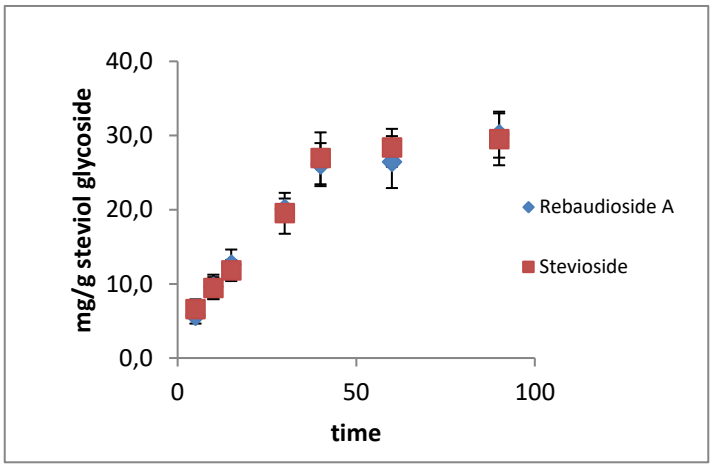

Figure 6. Steviol glycosides extraction kinetics. Each point represents the average value of three experiments; bars represent standard deviations.

3.3 Central composite design

RSM was used to evaluate the influence of some variables on steviol glycosides extraction. In particular, % of water, sonication amplitude, and temperature were chosen as independent variables. The sonication amplitude control of the processor allowed for setting the ultrasonic vibration at the probe at any desired level between 32–82% (with a range 20–100% for α values in CCD) of the nominal power. As water concerns, having used in kinetic study 50% of water which was useful to increase the extraction efficiency, the range 18–42% (with a range 9.8–50.2% for α values in CCD) was chosen in RSM with the aim of reducing as much as possible the water content. Lòpez-Carbon et al. reported 75 °C as the optimal temperature for steviol glycosides extraction [4]. Therefore, temperature values ranging between 35–65 °C (with a range 25–75 °C for α values in CCD) were chosen. The responses obtained by HPTLC analysis for each of the 20 experimental points are listed in Table 1. The predicted model can be described by the following second-order polynomial equations:

$Y_1 = -49.0727 + 1.79784*X_1 + 0.346136*X_2 + 1.28873*X_3 - 0.0279728*X_1^2 + 0.0281667*X_1*X_2 - 0.0280167*X_1*X_3 - 0.0110436*X_2^2 + 0.00568*X_2*X_3 - 0.00365892*X_3^2$

$Y_2 = -22.2866 + 0.872493*X_1 + 0.328113*X_2 + 1.11326*X_3 - 0.0180648*X_1^2 + 0.0332361*X_1*X_2 - 0.029575*X_1*X_3 - 0.0120643*X_2^2 + 0.00402*X_2*X_3 - 0.0009066*X_3^2$

where Y_1 is the stevioside concentration (mg/g *Stevia*) and Y_2 is the rebaudioside A concentration (mg/g *Stevia*).

Table 1. Box-Behnken design of process variables along with observed values for the Y response.

Treatment runs	Coded variables			Process variables			HPTLC Responce mg/g			
	x_1[a]	x_2[b]	x_3[c]	Water %	T °C	Amplitude %	Y_1[d]	SD[e]	Y_2[f]	SD[e]
1	0	–α	0	30	24,77	57	24,7	2,4	31,3	2,1
2	+1	+1	–1	42	65	32	40,7	2,3	46,5	1,6
3	+1	+1	+1	42	65	82	60,1	4,2	63,4	4,4
4	0	0	+α	30	50	99,04	47,7	1,7	56,0	1,3
5	0	0	0	30	50	57	41,1	0,4	45,7	1,0
6	0	+α	0	30	75,23	57	37,5	1,8	39,9	3,6
7	0	0	0	30	50	57	41,0	2,9	45,3	1,1
8	+α	0	0	50,18	50	57	19,9	0,5	27,4	2,1
9	+1	–1	+1	42	35	82	15,6	0,9	20,3	1,5
10	0	0	0	30	50	57	42,1	0,1	45,3	0,4
11	–1	–1	+1	18	35	82	47,0	2,3	58,9	0,9
12	+1	-1	-1	42	35	32	31,4	0,9	33,5	2,3
13	–α	0	0	9,818	50	57	35,5	0,9	46,5	0,5
14	–1	–1	–1	18	35	32	11,1	0,4	20,0	1,2
15	0	0	–α	30	50	14,96	19,7	1,6	28,9	0,7
16	–1	+1	+1	18	65	82	50,6	2,2	60,0	3,4
17	–1	+1	–1	18	65	32	25,5	2,3	31,5	3,3
18	0	0	0	30	50	57	42,0	0,5	45,7	1,0
19	0	0	0	30	50	57	42,1	1,9	44,9	0,9
20	0	0	0	30	50	57	41,6	0,6	45,1	1,2

[a] X_1 is water (%); [b] X_2 is temperature (°C); X_3 is the amplitude (%), in section 3.3 are explained the level chosen for each one code variable; [d] Y_1 is stevioside concentration (mg/g *Stevia*); [e] SD is the standard deviation; [f] Y_2 is rebaudioside concentration (mg/g *Stevia*).

ANOVA data for stevioside and rebaudioside A are shown on a Pareto Chart (Figure 7), which represents the significant effects of all variables (linear and quadratic) and their interactions. Positive and negative effects of the factors in the response variable are represented by horizontal

bars while the dashed line represents the minimal magnitude of statistically significant effect (95% of the confidence interval) with respect to the response.

Both the response values were significantly affected by the linear terms amplitude and temperature ($p < 0.05$) and, to a lesser extent, by the cross-product term between temperature and % of water ($p = 0.026$). The greater effect of amplitude is certainly due to the ability of ultrasound irradiation, transmitted via solvent, to damage cell walls, thus improving metabolite diffusion. Hence, the higher the ultrasound irradiation power, the higher the extraction yields [31]. On the other hand, higher extraction temperatures reduce the viscosity of the extraction medium thus improving the extraction performance. The well-known positive effects of cavitation bubble collapsing on the surface of the leaves associated with increased temperatures have been previously reported in the literature [3].

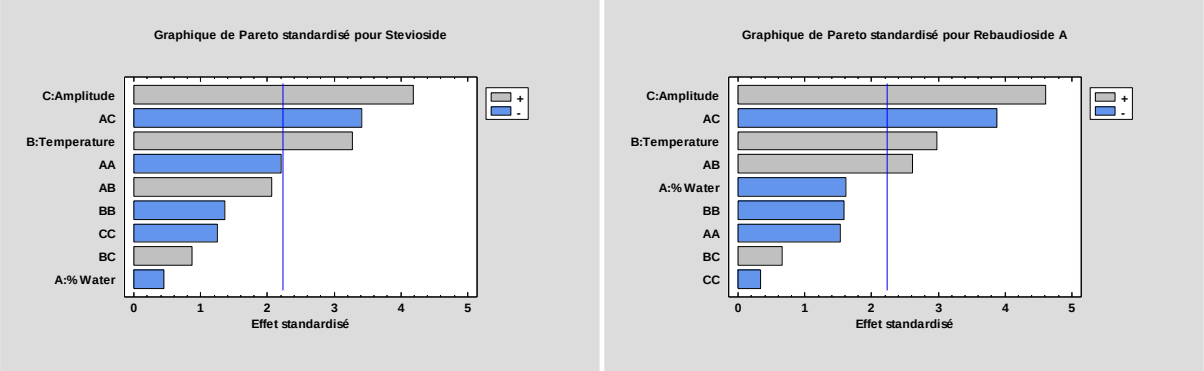

Figure 7. Standardized Pareto chart for stevioside (left) and rebaudioside A (right).

3.4 Comparison study between UAE and conventional extraction

Based on the quadratic model, the calculated optimum conditions for the ultrasound-assisted extraction of steviol glycosides from *Stevia* leaves were as follows: water content, 10%; temperature, 59.4 °C; amplitude, 90%. Thus, the extraction was carried out under these conditions and, with the aim of evaluating the influence of sonication on the extraction process, a conventional extraction was also performed at the same temperature and using the same water content. The quantities of extracted steviol glycosides were quantified by HPTLC and expressed as mg per gram of *Stevia* leaves (Figure 8). In particular, 14.21 ± 0.21 mg/g of stevioside and 21.4 ± 1.3 mg/g of

rebaudioside A were obtained after 10 min of sonication, with these values overlapping those obtained in 70 min of extraction (15.6 ± 0.7 mg/g and 20.1 ± 0.7 mg/g, respectively). Furthermore, after 40 min of sonication the amounts of stevioside and rebaudioside A obtained were 38 ± 0.1 mg/g and 45.1 ± 1.7 mg/g, respectively, demonstrating the powerful and the efficiently of DES-UAE proposed for steviol glycosides extraction. In addition, under the same extraction time and with a green solvent, the stevioside content obtained is four-fold higher than that the value reported by Rohuani [31]. Can we affirm that, the extractive method proposed is better than the method proposed recently by Rohuani. Moreover, comparing the quantities obtained with both techniques at the same time (70 min), the amount of steviol glycosides extracted by sonication was almost three times greater than that obtained by conventional extraction. Both results clearly demonstrate the usefulness of the ultrasonic effect, which was the only difference between the two experiments. The increased extraction efficiency is due to the cavitation as well as thermal effects resulting in cell wall disruptions, particle size reduction, and enhanced mass transfer across cell membrane.

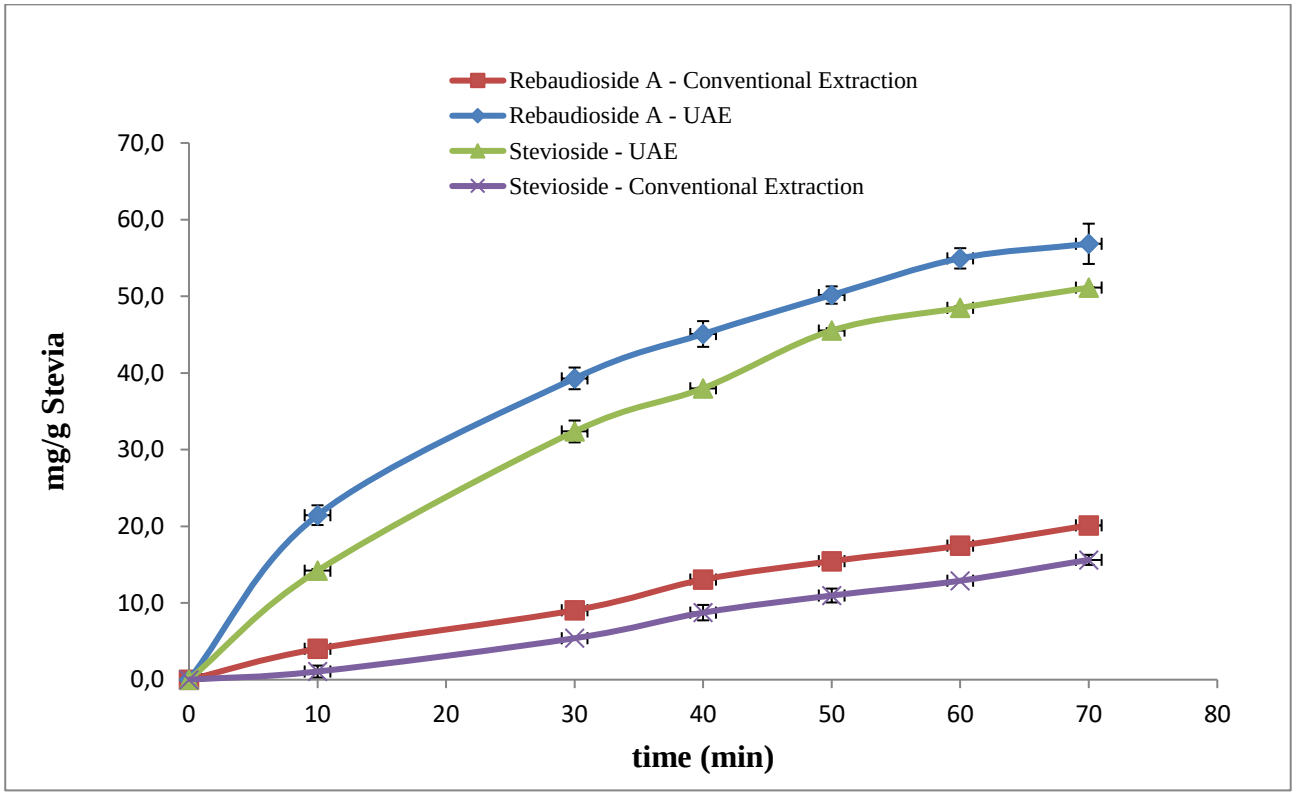

Figure 8. Steviol glycosides extracted by ultrasound-assisted extraction and conventional extraction.

3.5 Process impact on Stevia leaf structures

In order to verify the impact of ultrasounds on *Stevia* leaves, localized sonication and macroscopic investigation were carried out. Localized sonication was performed at 59.4 ± 1 °C, 90% sonication amplitude, using TEAC:EG with 10% of water, and placing the probe 0.5 cm from the leaf. A stereomicroscope was used to examine the ultrasound effects. As can be seen in Figure 9, the alteration of cell structures caused by ultrasounds increases with increasing time, with the leaf surface damage being maximum in 3 min. At this time, the leaf tissues have lost their shape and show numerous breakdowns. These effects stem from the well-known cavitation process: the micro-bubbles formed inside the medium grow and collapse on a solid surface, generating micro-jets and

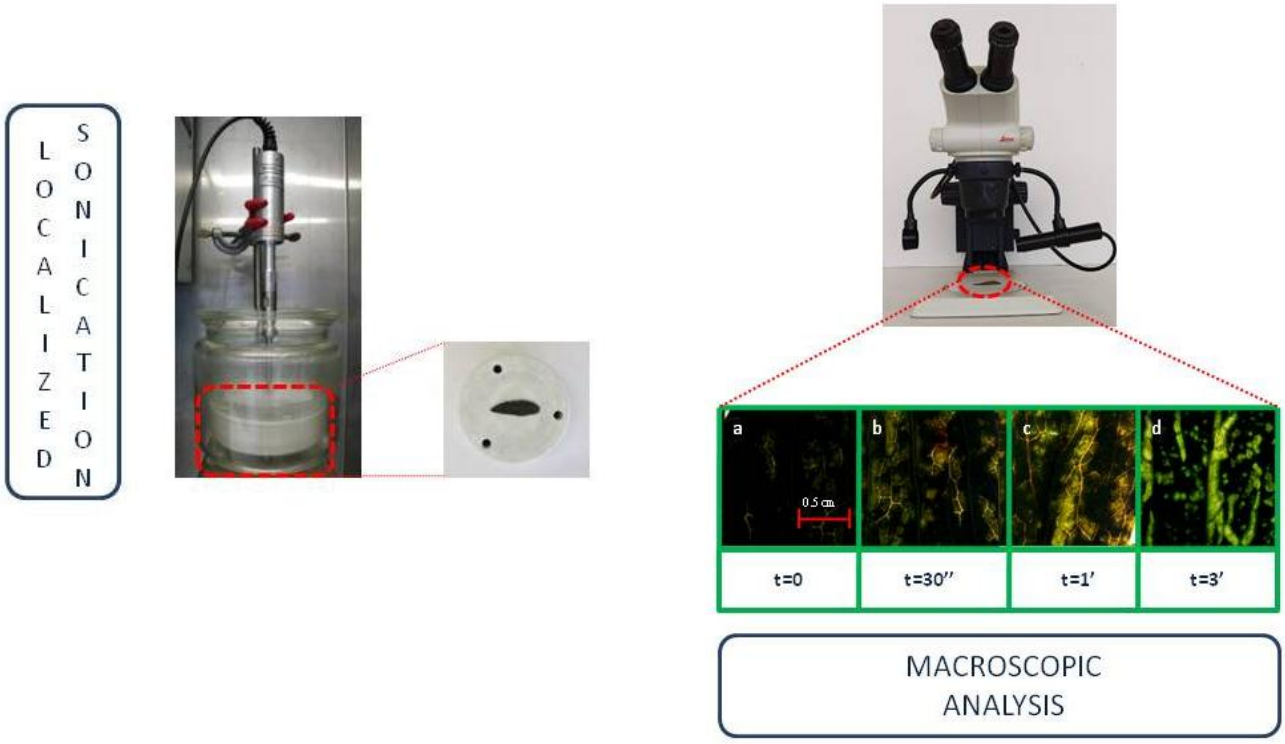

shock waves that determine erosion and fragmentation processes [32,33].

Figure 9. Experimental procedure: localized sonication and macroscopic investigation of *Stevia* leave structural modifications.

3.6 Proposition of a reaction mechanism

The plant extraction process can be described by thermodynamics or mass transfer mechanism which engenders a kinetic curve, as shown in Figure 8 [34]. Mass transfer depends on the wettability, defined by Brannan et al. as 'the affinity of a fluid for a solid'[35], thus highlighting the pivotal role of the solvent in the extraction process. The wettability of a solid can be evaluated measuring the contact angle (CA, θ) of a liquid on the solid surface; CA values ranging between 0–90° indicate a good wettability, as opposed to CA values greater than 90°. In the present study, three different solvents were used for CA determination at 25 °C, namely TEAC:EG (molar ratio 1:2), TEAC:EG with 10% water, and water (Figure 10). The CA of water on dried *Stevia* leaves was 64°. The positive effect of water added to TEAC:EG was corroborated, with the CA being decreased from 75° to 71° when water increased to 10%.

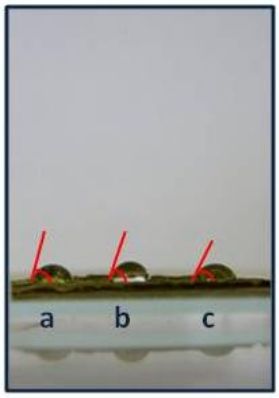

Figure 10. Angle of conctact investigation. **(a)** Tetraethylammonium Chloride : Ethylene glycol; **(b)** Tetraethylammonium Chloride : Ethylene glycol + 10% Water; **(c)** Water.

Bondarev et al. [35] reported that the epidermal structure of *Stevia* leaves is characterized, on both adaxial and abaxial leaf surfaces, by large trichomes, small trichomes, and glands, which represent the reserve of steviol glycosides. On the other hand, it is well known that in fruits and roots the solutes are distributed inside the solid matrix, whereas in flowers and leaves solutes are inside the

trichomes. Solid-liquid extraction is influenced by different parameters such as porosity and pore tortuosity, that can reduce the transport of the internal compounds towards the surrounding medium. [36] In the kinetic curve of UAE (Figure 8), three stages can be described: a constant extraction rate period (CER, 0–10 min), a falling extraction rate period (FER, 10–40 min), and a diffusion-controlled rate period (DC, 40–70 min) [37]. We suppose that the extraction of steviol glycosides could stem from the changes in the structure of the cells *Stevia* leaves ~~cells~~ arising from the presence of DES. In fact, to dissolve steviol glycosides, a DES solvent has to penetrate and destabilize the cell structure. In the first stage, DES molecules self-aggregate on the cell wall, with a reduction of surface forces at the interface that improves the cell wall's wettability. Subsequently, DES and water molecules can penetrate easily into ~~the cell *Stevia* structure and access~~ the cell membrane. The penetration of DES into the cell wall and membrane structure probably induces molecular disorganization and alters the permeability of the membrane facilitating the solubilization of steviol glycosides ~~molecules~~ (Figure 11). [38]

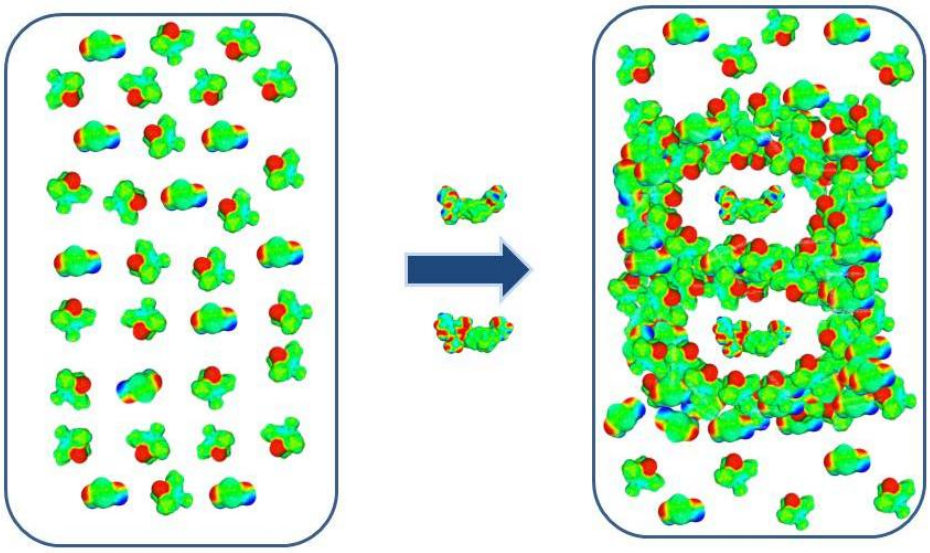

Figure 11. Cartoon representation of DES self-aggregation around rebaudioside A (under the arrow and down in the right panel) and stevioside (over the arrow and up in the right panel), to explain the steviol glycosides solubilization process.

Moreover, in the CER stage the ultrasound waves induce a longitudinal displacement of the solvent molecules which enhance the mass transfer of steviol glycosides, adsorbed on the matrix surface, into the solvent. Therefore, the highest extraction rate is reached, with surface phenomena occurring. In FER stage the pivotal role is played by the cavitation phenomena resulting from successive cycles of compression and rarefaction of the solvent molecules. During the rarefaction phase, the liquid experiences reduced pressure which generates a small cavity growing on successive rarefaction cycles, the cavitation bubble. After a few acoustic cycles, the bubble collapses onto the solid surface with the generation of microjets and shock waves responsible for the erosion and fragmentation of the matrix surface. Therefore, the solvent diffusion into the solid matrix is enhanced by ultrasound waves and the attractive forces holding the glycosides to the matrix are reduced. On the other hand, the superficial tissue disruption and macroscopic erosion have been demonstrated through the localized sonication study (Figure 12). Finally, the extraction rate decreases in the DC stage when the small amounts of residual solutes are extracted. Obviously, since no cavitation occurs in conventional extraction, the steviol glycosides content is lower than UAE at each stage of the extraction process. It is worth noting that steviol glycoside dissolution might be further favored by the presence of TEAC, representing the HBA in the DES we used, through the formation of hydrogen bonds with hydroxyl groups of stevioside and rebaudioside A, thus highlighting the success of the combination DES-UAE.

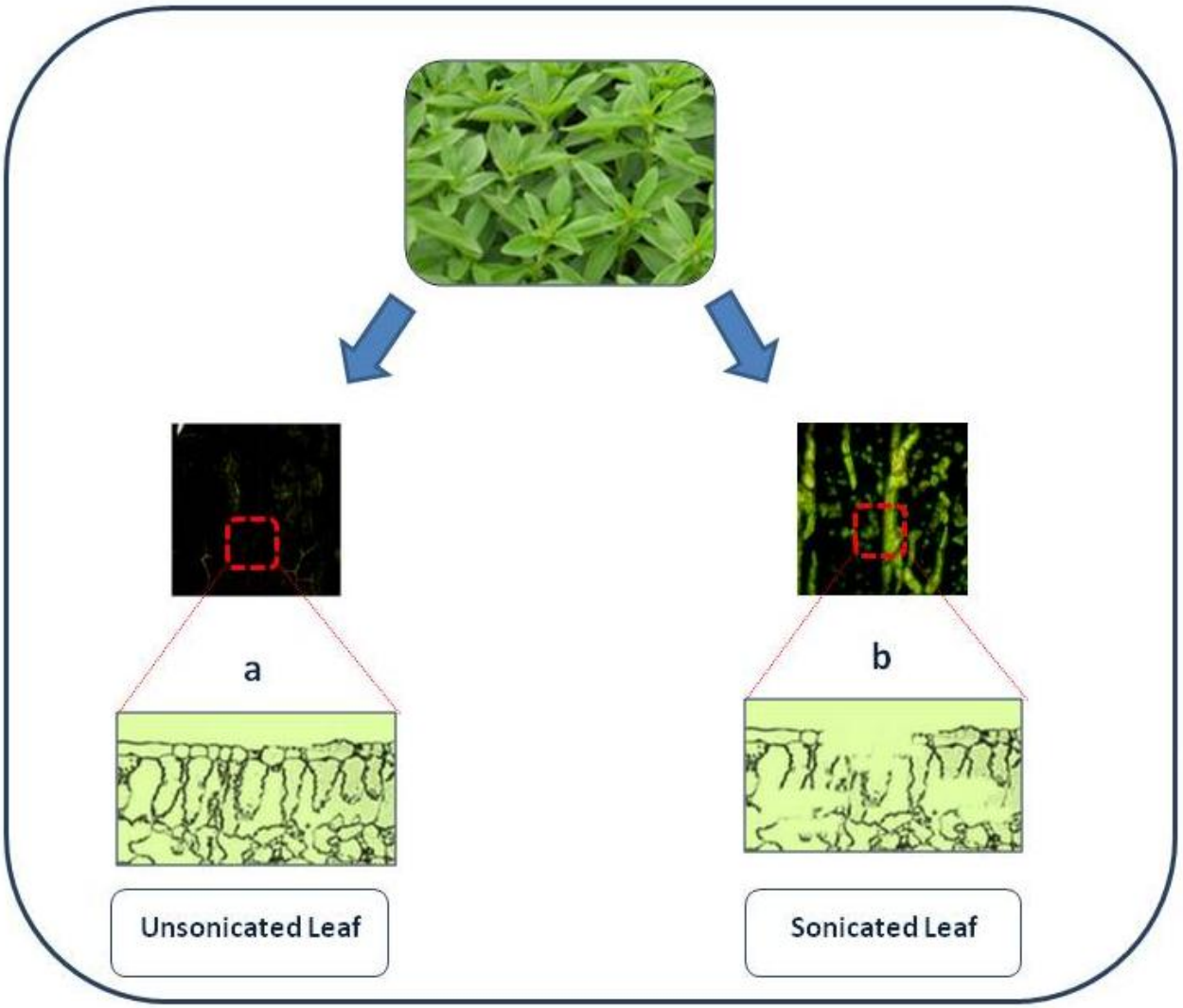

422 **Figure 12.** Investigation of *Stevia rebaudiana* leaf surface. (a) Visualization of the leaf before the
423 sonication treatment; (b) visualization after 3 min of localized sonication treatment with proposed
424 mechanism.

425 **4. Conclusions**

426 In the present study, a green and efficient DES-UAE was developed to extract stevioside and
427 rebaudioside A from *Stevia rebaudiana* Bertoni. A COnductor-like Screening MOdel for real
428 solvent was used to predict the solubility indices for the selected solutes (stevioside, rebaudioside
429 A, B, C, D, E, F) in 26 different solvents and TEAC:EG has been chosen as the extraction solvent.
430 Furthermore, the response surface methodology has been applied to optimize the stevioside and
431 rebaudioside A extraction conditions which were 59.4 °C, 70 min, 90% amplitude, and TEAC:EG

(in molar ratio 1:2) with 10% of water. Under these conditions, the glycoside amount obtained by UAE was almost three times higher than that obtained by conventional extraction. Moreover, the DES-UAE method proposed is more efficiently than that recently reported by Rouhani [31]. A macroscopic investigation of sonicated and non-sonicated leaves was further carried out to demonstrate the impact of ultrasound waves on *Stevia* leaves. In conclusion, this study demonstrates for the first time the excellent synergism between DES and ultrasound in glycoside extraction from *Stevia rebaudiana* Bertoni.

Conflicts of interest

There are no conflicts to declare.

Credit author statement

Milani Gualtiero performed data curation, investigation and writing–original draft preparation. Maryline Vian performed methodology, software and validation. Maria Maddalena Cavalluzzi performed visualization. Carlo Franchini performed writing–review & editing. Filomena Corbo performed writing–review & editing. Giovanni Lentini performed supervision and visualization. Farid Chemat performed conceptualization, supervision and validation.

References

[1] R. Lemus-Mondaca, A. Vega-Gálvez, L. Zura-Bravo, K. Ah-Hen, *Stevia rebaudiana* Bertoni, source of a high-potency natural sweetener: a comprehensive review on the biochemical, nutritional and functional aspects, Food Chemistry, 132 (2012) 1121–1132. https://doi.org/10.1016/j.foodchem.2011.11.140.

[2] U. Wölwer-Rieck, The leaves of *Stevia rebaudiana* (Bertoni), their constituents and the analyses there of: a review, Journal of Agricultural and Food Chemistry, 60 (2012) 886–895. https://doi.org/10.1021/jf2044907.

[3] J.Š. Žlabur, S. Voća, N. Dobričević1, M. Brnčić, F. Dujmić, S.R. Brnčić, Optimization of ultrasound assisted extraction of functional ingredients from *Stevia rebaudiana* Bertoni leaves, International Agrophysics, 29 (2015) 231-237. https://doi.org/10.1515/intag-2015-0017.

[4] V. López-Carbón, A. Sayago, R. González-Domínguez, Á. Fernández-Recamales, Simple and efficient green extraction of steviol glycosides from *Stevia rebaudiana* leaves, Foods, 8 (2019) 1–10. https://doi.org/10.3390/foods8090402.

[5] M.F. Hossain, M.T. Islam, M.A. Islam, S. Akhtar, Cultivation and uses of *Stevia* (*Stevia rebaudiana* Bertoni): a review, African Journal of Food, Agriculture, Nutrition and Development, 17 (2017) 12745-12757. https://doi.org/10.18697/ajfand.80.16595.

[6] F. Chemat, N. Rombaut, A.S. Fabiano-Tixier, J.T. Pierson, A. Bily, Green extraction: from concepts to research, education, and economical opportunities in: F. Chemat, J. Strube (Eds.), Green extraction of natural products: theory and practice, Wiley-VCH Verlag GmbH & Co., Weinheim, 2015, pp 1–30.

[7] F. Chemat, M.A. Vian, G. Cravotto, Green extraction of natural products: concept and principles, International Journal of Molecular Sciences, 13 (2012) 8615–8627. https://doi.org/10.3390/ijms13078615.

[8] G. Milani, F. Curci, M.M. Cavalluzzi, P. Crupi, I. Pisano, G. Lentini, M.L. Clodoveo, C. Franchini, F. Corbo, Optimization of microwave-assisted extraction of antioxidants from bamboo shoots of *Phyllostachys pubescens*, Molecules, 25 (2020) 1–11. https://doi.org/10.3390/molecules25010215.

[9] C. Bruno, G. Lentini, A. Catalano, A. Carocci, A. Lovece, A. Di Mola, M.M. Cavalluzzi, P. Tortorella, F. Loiodice, G. Iaccarino, P. Campiglia, E. Novellino, C. Franchini, Microwave-assisted synthesis of KN-93, a potent and selective inhibitor of Ca^{2+}/calmoduline-dependent protein kinase II, Synthesis, 24 (2010) 4193-4198. https://doi.org/10.1055/s-0030-1258298.

[10] L. Caputo, L. Quintieri, M.M. Cavalluzzi, G. Lentini, S. Habtemariam, Antimicrobial and antibiofilm activities of citrus water-extracts obtained by microwave-assisted and conventional methods, Biomedicines, 6 (2018) 1–14. https://doi.org/10.3390/biomedicines6020070.

[11] M.L. Clodoveo, V. Moramarco, A. Paduano, R. Sacchi, T. Di Palmo, P. Crupi, F. Corbo, V. Pesce, E. Distaso, P. Tamburrano, R. Amirante, Engineering design and prototype development of a full scale ultrasound system for virgin olive oil by means of numerical and experimental analysis, Ultrasonics Sonochemistry, 37 (2017) 169–181. https://doi.org/10.1016/j.ultsonch.2017.01.004.

[12] G. Cravotto, P. Cintas, Power ultrasound in organic synthesis: moving cavitational chemistry from academia to innovative and large-scale applications, Chemical Society Reviews, 35 (2006) 180–196. https://doi.org/10.1039/b503848k.

[13] G. Haar, Therapeutic applications of ultrasound, Progress in Biophysics and Molecular Biology, 93 (2007) 111–129. https://doi.org/10.1016/j.pbiomolbio.2006.07.005.

[14] L. Cecchi, M. Bellumori, F. Corbo, G. Milani, M.L. Clodoveo, N. Mulinacci, Implementation of the sono-heat-exchanger in the extra virgin olive oil extraction process: end-user validation and analytical evaluation, Molecules, 24 (2019) 1–13. https://doi.org/10.3390/molecules24132379.

[15] T.J. Mason, J.P. Lorimmes, General principles, in: T.J. Mason, J.P. Lorimmes (Eds.), Applied sonochemistry, uses of power ultrasound in chemistry and processing, Wiley-VCH Verlag GmbH & Co., Weinheim, 2002, pp 25–72.

[16] A.K. Dwamena, Recent advances in hydrophobic deep eutectic solvents for extraction, Separations, 6 (2019)1–15. https://doi.org/10.3390/separations6010009.

[17] M. Vian, C. Breil, L. Vernes, E. Chaabani, F. Chemat, Green solvents for sample preparation in analytical chemistry, Current Opinion in Green and Sustainable Chemistry, 5 (2017) 44–48. https://doi.org/10.1016/j.cogsc.2017.03.010.

[18] L. Benvenutti, A.A. Ferreira Zielinski, S.R.S. Ferreira, Which is the best food emerging solvent: IL, DES or NADES?, Trends in Food Science & Technology, 90 (2019) 133–146. https://doi.org/10.1016/j.tifs.2019.06.003.

505 [19] M.A. Farajzadeh, M.R.A. Mogaddam, M. Aghanassab, Deep eutectic solvent-based dispersive
506 liquid–liquid microextraction, Analytical Methods, 8 (2016) 2576–2583.
507 https://doi.org/10.1039/C5AY03189C.
508 [20] Z. Meng, J. Zhao, H. Duan, Y. Guan, L. Zhao, Green and efficient extraction of four bioactive
509 flavonoids from *Pollen Typhae* by ultrasound-assisted deep eutectic solvents extraction, Journal of
510 Pharmaceutical and Biomedical Analysis, 161 (2018) 246–253.
511 https://doi.org/10.1016/j.jpba.2018.08.048.
512 [21] Y.H. Hsieh, Y.Li, Z. Pan, Z. Chen, J. Lu, J. Yuan, Z. Zhu, J. Zhang, Ultrasonication-assisted
513 synthesis of alcohol-based deep eutectic solvents for extraction of active compounds from ginger,
514 Ultrasonics Sonochemistry, 63 (2019) 1–25. https://doi.org/10.1016/j.ultsonch.2019.104915.
515 [22] M. Xu, L. Ran, N. Chen, X. Fan, D. Ren, L. Yi, Polarity-dependent extraction of flavonoids
516 from citrus peel waste using a tailor-made deep eutectic solvent, Food Chemistry, 297 (2019) 1–10.
517 https://doi.org/10.1016/j.foodchem.2019.124970.
518 [23] S.E.E. Warrag, I. Adeyemi, N.R. Rodriguez, I.M. Nashef, M.S. Annaland, M.C. Kroon, C.J.
519 Peters, Effect of the type of ammonium salt on the extractive desulfurization of fuels using deep
520 eutectic solvents, Journal of Chemicals & Engineering Data, 63 (2018) 1088−1095.
521 https://doi.org/10.1021/acs.jced.7b00832.
522 [24] S. Mulyono, H.F. Hizaddin, I. M. Alnashef, M. A. Hashim, A. H. Fakeeha, M. K. Hadj-Kali,
523 Separation of BTEX aromatics from n-octane using a (tetrabutylammonium bromide + sulfolane)
524 deep eutectic solvent – experiments and COSMO-RS prediction, RSC Advances, 4 (2014) 17597–
525 17606. https://doi.org/10.1039/C4RA01081G.
526 [25] H. K. Ravi, C. Breil, M.A. Vian, F. Chemat, P.R. Venskutonis, Biorefining of bilberry
527 (*Vacciniummyrtillus L.*) pomace using microwave hydrodiffusion and gravity, ultrasound-assisted,
528 and bead-milling extraction, ACS Sustainable Chemistry & Engineering, 6 (2018) 4185–4193.
529 https://doi.org/10.1021/acssuschemeng.7b04592.

530 [26] F. Eckert, A. Klamt, Fast solvent screening via quantum chemistry: COSMO-RS approach,
531 American Institute of Chemical Engineers Journal, 48 (2002) 369–385.
532 https://doi.org/10.1002/aic.690480220.
533 [27] S. Benamid, Y. Benguarda, I.M. Nashef, N. Haddaoui, Theoretical study of physicochemical
534 properties of selected ammonium salt-based deep eutectic solvents; Journal of Molecular Liquids,
535 285 (2019) 38–46. https://doi.org/10.1021/ef5028873.
536 [28] M. Yizhak, The variety of deep eutectic solvents, in: M. Yizhak (Eds.), Deep eutectic solvents,
537 Springer Nature Switzerland AG, 2019, pp 13–44.
538 [29] M. Yizhak, Properties of deep eutectic solvents, in: M. Yizhak (Eds.), Deep eutectic solvents,
539 Springer Nature Switzerland AG, 2019, pp 45–110.
540 [30] H.F. Hizaddin, A. Ramalingam, M.A. Hashim, M.K.O. Hadj-Kali, Evaluating the performance
541 of deep eutectic solvents for use in extractive denitrification of liquid fuels by the conductor-like
542 screening model for real solvents, Journal of Chemicals & Engineering Data, 59 (2014) 3470−3487.
543 https://doi.org/10.1021/je5004302.
544 [31] M. Rouhani, Modeling and optimization of ultrasound-assisted green extraction and rapid
545 HPTLC analysis of stevioside from *Stevia Rebaudiana*, Industrial Crops and Products, 132 (2019)
546 226–235. https://doi.org/10.1016/j.indcrop.2019.02.029.
547 [32] J. Jian-bing, L. Xiang-hong, C. Mei-qiang, X. Zhi-chao, Improvement of leaching process of
548 Geniposide with ultrasound, Ultrasonics Sonochemistry, 13 (2006) 455–462.
549 https://doi.org/10.1016/j.ultsonch.2005.08.003.
550 [33] F. Chemat, V. Tamao, M. Virot, Ultrasound-assisted extraction in food analysis, in:
551 SemihÖtles (Eds.), Handbook of food analysis instruments, Taylor & Francis Group, LLC, 2009, pp
552 85–103.
553 [34] M. Palma, G.F. Barbero, Z. Pineiro, A. Liazid, C.G. Barroso, M.A. Rostagno, J.M. Prado,
554 M.A.A. Meireles, Extraction of natural products: principles and fundamental aspects, in: M.A.

555 Rostagno, J.M. Prado (Eds.), Natural product extraction: principles and applications, The Royal
556 Society of Chemistry, 2013, pp 58–88.
557 [35] N.I. Bondarev, M.A. Sukhanova, G.A. Semenova, O.V. Goryaeva, S.E. Andreeva, A.M.
558 Nosov, Morphology and ultrastructure of trichomes of intact and in vitro plants of *Stevia*
559 *Rebaudiana* Bertoni with reference to biosynthesis and accumulation of steviol glycosides, Moscow
560 University Biological Sciences Bulletin, 65 (2010) 12–16.
561 https://doi.org/10.3103/S0096392514030110.
562 [36] F. Chemat, A.S. Fabiano-Tixier, M.A. Vian, T. Allaf, E. Vorobiev, Solvent-free extraction of
563 food and natural product, Trends in Analytical Chemistry, 71 (2015) 157–168.
564 http://dx.doi.org/10.1016/j.trac.2015.02.021
565 [37] A.Y. Aydar, V. Rodriguez-Martinez, B.E. Farkas, Determination and modeling of contact
566 angle of *Canola* oil and olive oil on a PTFE surface at elevated temperatures using air or steam as
567 surrounding media, Food Science and Technology, 65 (2016) 304–310.
568 http://dx.doi.org/10.1016/j.lwt.2015.08.022.
569 [38] G. Raman, V.G. Gaikar, Extraction of Piperine from *Piper nigrum* (Black Pepper) by
570 Hydrotropic Solubilization, Industrial & Engineering Chemistry Research, 41 (2002) 2966-2976.
571 http://dx.doi.org/10.1021/ie0107845
572